Journal of Thermal Analysis, Vol. 34 (1988) 1335–1347

SYNTHESIS, SPECTRAL STUDY AND THERMAL BEHAVIOUR OF SOME 4-(O-ACETYL)-GLYCOPYRANOSYLAMINO-5-NITROSOPYRIMIDINE DERIVATIVES

M. Nogueras[+], *R. López*, *Mª. Dolores Gutierrez* and *A. Sánchez*

DEPT. DE QUIMICA ORGÁNICA E INORGÁNICA,
COLEGIO UNIVERSITARIO DE JAÉN, UNIVERSIDAD DE GRANADA,
23071 JAÉN, SPAIN

(Received November 4, 1987)

The syntheses, specific optical rotations, spectral features (^{1}H–NMR, UV-visible and IR spectroscopy) and thermal characterization of seven 4-(O-acetyl)-glycopyranosylamino-5-nitrosopyrimidine derivatives are reported. With IR spectroscopy, the starting of the pyrolytic decomposition mechanism of the compounds was established.

In view of the biological roles of pyrimidines, their nucleosides and nucleotides [1–5] and some of their metal complexes [3, 6], we have focused our interest on the study of pyrimidine derivatives and some of their nucleoside and nucleotide analogues.

We recently carried out spectral and thermal studies on the following compounds: a) A series of seven 4-glycosylamino-6-oxopyrimidine derivatives [7]. b) The corresponding 4-glycopyranosylamino-5-nitroso-6-oxopyrimidine derivatives [8]. c) A series of seven 4-(O-acetyl)-glycopyranosylamino-6-oxopyrimidine homologues of the compounds in section a) [9].

As a follow-up in the present paper we report studies on the seven 4-(O-acetyl)-glycopyranosylamino-5-nitroso-6-oxopyrimidine homologues of the section c) compounds, whose general structures are shown in Scheme I.

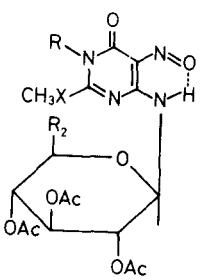

[+] Author for correspondence.

John Wiley & Sons, Limited, Chichester
Akadémiai Kiadó, Budapest

Experimental

Microanalyses of C. H. and N were performed at the Instituto Nacional de Química Orgánica (CSIC, Madrid). Specific optical rotations were measured with a Perkin–Elmer 141 polarimeter.

^{1}H–NMR spectra were obtained with a Perkin–Elmer R–600 spectrophotometer, in $CDCl_3$ and DMSO–d_6 as solvents. IR spectra were recorded with a Beckman 4250 spectrophotometer using KBr pellets, and UV-visible spectra with a Beckman 25 spectrophotometer using aqueous solutions of the samples.

DSC plots were obtained with a Mettler DSC–20 differential scanning calorimeter at a heating rate of 10 deg/min^{-1}, using samples of 1.409–4.496 mg. Thermogravimetric curves were obtained with a Mettler TG 50 thermobalance in a static pure air atmosphere, at a heating rate of 10 deg/min^{-1}, with samples of 4.550–14.001 mg.

Results and discussion

The seven compounds under study were synthesized by suspending 5 mmole of the corresponding 4-(O-acetyl)-glycopyranosylamino-6-oxopyrimidine precursor in 4 ml of acetic acid and heating the resulting mixture until dissolution was achieved, after which 6 mmole of $NaNO_2$ was added. The resulting blue solutions were kept stirred for 15 minutes, then poured into cold water and left for 24 hours. The resulting blue solids were filtered off and washed with cold water. The products obtained were recrystallized from ethanol.

To obtain the 4-(O-acetyl)-glycopyranosylamino-6-oxopyrimidine precursor derivatives, a previously reported method was used [10].

The colours, yields, specific optical rotations and analytical data on the compounds are listed in Table 1.

All the compounds are coloured, due to the presence of the 5-NO chromophore group in their molecules. Table 1 reveals the good agreement between the found analytical data and those calculated from the formulae. The data show that all the compounds are anhydrous.

Spectral data

Visible and UV spectral data on the compounds are given in Table 2. The expected NO chromophore bands in the visible arise in the range 602–630, in accordance with the colour of the compounds. The bands observed in the UV range are those characteristic of pyrimidine derivatives, all of them assignable to $\pi \rightarrow \pi^*$

Table 1 Yields, specific optical rotations and analytical data on the compounds

Compound	Yield, %	D, (c 1, DMSO)	Formula	Analytical data, %		
				C	H	N
A	80	+0.2	$C_{19}H_{24}N_4O_{12}$	45.60 (45.58)	4.83 (4.80)	11.20 (11.00)
B	83	+0.0	$C_{17}H_{22}N_4O_{10}$	46.15 (46.28)	5.01 (5.01)	12.67 (12.58)
C	96	+0.2	$C_{20}H_{26}N_4O_{12}$	46.69 (46.50)	5.09 (4.98)	10.89 (10.72)
D	92	+0.5	$C_{16}H_{20}N_4O_9S$	43.24 (43.22)	4.54 (4.75)	12.61 (12.58)
E	81	+0.1	$C_{19}H_{24}N_4O_{11}S$	44.15 (43.70)	4.68 (4.81)	10.85 (10.45)
F	83	+0.1	$C_{17}H_{22}N_4O_9S$	44.53 (44.16)	4.84 (4.91)	12.22 (12.24)
G	89	+0.9	$C_{20}H_{26}N_4O_{11}S$	45.27 (45.28)	4.94 (4.90)	10.56 (10.57)

Calculated analytical values in parentheses.

transitions [11–17]. Possible forbidden $n \rightarrow \pi^*$ transitions have not been observed, most probably because of their negligible intensities at the working concentration values (see Table 2); furthermore, they are probably hidden by the strong $\pi \rightarrow \pi^*$ bands [16, 18].

The most significant IR spectral bands of the compounds are detailed in Table 3.

The ν(NH) bands appear in the range 3000–3480 cm^{-1}. The broadening of such bands is due to the probable involvement of the 4-NH groups in hydrogen-bonding interactions. The ν(C=O) stretching vibration bands due to acetate groups have been assigned by comparing the IR spectra of the compounds under study with those of the 4-glycopyrano-sylamino-5-nitroso-6-oxopyrimidine homologues, which were discussed previously [8]. These bands appear in the range 1745–1755 cm^{-1}, and are clearly different from the ν(C=O) stretching vibration bands of the pyrimidine ring C=O group. The latter appear in a lower range (1685–1700 cm^{-1}), in accordance with the relatively aromatic character of the pyrimidine ring. The ν(N—O) stretching vibrations bands were assigned by comparing the spectra under study with those corresponding to the 4-(O-acetyl)-glycopyranosylaminopyrimidine homologues [9].

The occurrence of the ν(N—H), $\nu(C=O)_{cycle}$ and ν(NO) bands suggests the existence of the amino-ketone tautomeric form as the predominant form in the solid state. The remaining bands were assigned in accordance with previous reports concerning analogous compounds [7–11].

The ^{1}H-NMR data on the compounds are listed in Table 4.

The 1–CH_3, 1–H, O—CH_3 and 5–CH_3 signals are all in similar ranges to those found for analogous compounds previously reported [7–9]. The very low field values at which the C(1)–H and C(4)–NH signals appear in all of the spectra suggest a relatively mono- or biprotic acidic character of these compounds; this was proved by the fact that these signals disappeared from all of the spectra when D_2O was

added to the DMSO–d_6 solutions used to obtain them. As concerns the C(4)–NH amino group signals, it is interesting to point out that these are at similar values (between 12.20 and 13.05 ppm) to those for the corresponding 4-glycopyranosylamino-5-nitroso-6-oxopyrimidines [19–20], but they are appreciably higher than the values for the C(4)–NH signals of the homologous compounds without exocyclic substituents on C(5). This fact can be explained on the basis of the existence of intramolecular bridging interactions between the C(4)–NH and C(5)–NO groups, as shown in Scheme II. On the other hand, the signal of the

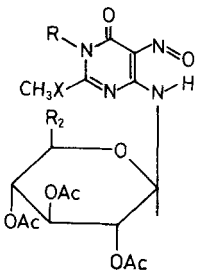

	X	R	R_2
A	O	H	CH_2OAc
B	O	CH_3	H
C	O	CH_3	CH_2OAc
D	S	H	H
E	S	H	CH_2OAc
F	S	CH_3	H
G	S	CH_3	CH_2OAc

C(4)–NH group under discussion appears as a doublet in all the spectra, due to the nuclear spin coupling of this hydrogen atom and the H-anomeric one, as proved by the fact that this signal becomes a singlet when the anomeric H atom is irradiated. Likewise, the signal due to H-anomeric (H–′) appears as a multiplet, but becomes a doublet ($J_{1',2'}$ = 8.2 Hz) when the C(4)–NH signal is irradiated. These facts indicate that the said multiplet signal is due to the simultaneous spin-spin coupling between the hydrogen nuclei of the C(4)–NH, H–1′ and H–2′ groups; nevertheless, under the above irradiation, only the coupling between H–1′ and H–2′ remains.

Thermal study

TG and DSC plots for the seven compounds under study appear in Figs 1 and 2, respectively. From these Figures, the thermal data shown in Table 5 were obtained.

Table 2 UV and visible data (solvent: MeOH)

Compound	Concentration mol × l^{-1}	λ_{max}, nm		Assignment
A	1.1×10^{-4}	228	18900	$\pi \rightarrow \pi^*$
		288	5250	$\pi \rightarrow \pi^*$
		336	12030	$\pi \rightarrow \pi^*$
	3.8×10^{-3}	602	56	chromophore
B	1.3×10^{-4}	229	18200	$\pi \rightarrow \pi^*$
		302(sh)	— —	$\pi \rightarrow \pi^*$
		336	12800	$\pi \rightarrow \pi^*$
	4.6×10^{-3}	603	59	chromophore
C	1.1×10^{-4}	228	18140	$\pi \rightarrow \pi^*$
		299(sh)	— —	$\pi \rightarrow \pi^*$
		337	12200	$\pi \rightarrow \pi^*$
	3.5×10^{-3}	604	56	chromophore
D	1.1×10^{-4}	225	12920	$\pi \rightarrow \pi^*$
		295	8830	$\pi \rightarrow \pi^*$
		350	18950	$\pi \rightarrow \pi^*$
	5.1×10^{-3}	626	55	chromophore
E	6.7×10^{-5}	224	13670	$\pi \rightarrow \pi^*$
		293	8210	$\pi \rightarrow \pi^*$
		351	17270	$\pi \rightarrow \pi^*$
	2.6×10^{-3}	629	54	chromophore
F	9.3×10^{-5}	221	13150	$\pi \rightarrow \pi^*$
		280	7240	$\pi \rightarrow \pi^*$
		318(sh)	— —	$\pi \rightarrow \pi^*$
		351	17960	$\pi \rightarrow \pi^*$
	4.6×10^{-3}	629	56	chromophore
G	6.2×10^{-5}	224	14370	$\pi \rightarrow \pi^*$
		281	7050	$\pi \rightarrow \pi^*$
		322(sh)	— —	$\pi \rightarrow \pi^*$
		351	15160	$\pi \rightarrow \pi^*$
	3.2×10^{-3}	630	54	chromophore

It can be seen that compounds C, E and G contain practically negligible ethanol amounts (1.30%, 1.15% and 1.19%, respectively). The corresponding desolvation energies (see Table 5) prove that the solvent molecules are probably retained by strong hydrogen-bonds.

Secondly, the fact should be noted that none of the compounds under examination fuse before the starting of their pyrolytic decomposition processes;

Table 3 IR spectral data

Compound	ν(NH)	ν(C—H)	$\nu(C=O)_{acet}$	$\nu(C=O)_{ring}$	$\nu(C=C)$ + $\nu(C=N)$	ν(NO)	$\nu(CH_3)_{sym}$	ν(C—N)	ν(C—O)	Skelet.	ν(C—S)
A	3200–3000m	2980w 2950w 2930w	1745s	1700m	1685s	1500m	1370m	1220s	1055m 1040m	785m	—
B	3470w	3020w 2950w 2870w	1755s	1710s	1595s 1560s	1490m	1370s	1245s 1210s	1065s 1045s	780m	—
C	3470w	3000w 2950w 2870w	1750s	1700m	1585s 1570s	1495m	1370m	1230s	1060m 1035m	780m	—
D	3240m 3210m 3180m	3040w 2950w 2920w 2880w	1740s	1700s	1600s 1520s	1470s	1360m	1275m 1245s 1220s	1085s 1065s 1030s	765m	595m
E	3200–3000w	3010w 2935w	1745s	1685s	1560s	1475m	1370m	1225s	1050s	780m	600m
F	3470w	3010w 2950w 2870w	1755s	1700s	1570s 1530s	1480m	1370m	1240s 1215s	1060s 1040s	775m	595m
G	3480w	3010w 2940w	1750s	1685s	1570s 1520s	1480m	1370m	1225s	1070s 1040s	780m	600m

s: strong, m: medium, w: weak.

Table 4 ^{1}H–NMR data on the compounds (ppm)

Compound	Solvent	CH_3–1	H–1	CH_3–O	CH_3–S	AcO—	C4–NH ($J_{NH,1}$, Hz)	H–1′ ($J_{1',2'}$, Hz)	Sugar
A	$CDCl_3$	—	12.2s broad	4.1s	—	2.1s 12H	12.4d (8.2)	5.6m + D_2O d (8.2)	5.4–4.8m 4H 4.3–3.7m 2H
	(DMSO)–d_6	—	13.0s broad	4.1s	—	2.0s 12H	12.5d (8.2)	5.9m + D_2O d (8.2)	5.7–4.8m 4H 4.4–3.9m 2H
B	$CDCl_3$	3.5s	—	4.2s	—	2.1s 3H 2.3s 3H 2.0s 3H	12.7d (8.2)	5.8st + D_2O d (8.2)	5.6–4.6m 3H 4.1–3.7m 2H
	(DMSO)–d_6	3.4s	—	4.2s	—	2.1s 3H 2.0s 3H 1.9s 3H	12.3d (8.2)	5.9m + D_2O d (8.2)	5.7–4.7m 3H 4.0–3.6m 2H
C	$CDCl_3$	3.5s	—	4.2s	—	2.1s 12H	12.4d (8.2)	5.7m + D_2O d (9)	5.6–4.8m 4H 4.2–3.7m 2H
	(DMSO)–d_6	3.4s	—	4.2s	—	2.0s 12H	12.2d (8.2)	6.0m + D_2O d (9.5)	5.8–4.7m 4H 4.4–3.9m 2H
D	$CDCl_3$	—	12.5s broad	—	2.6s	2.0s 3H 2.2s 6H	12.5d (8.2)	5.8st + D_2O d (8.2)	5.6–4.6m 3H 4.4–3.2m 2H
	(DMSO)–d_6	—	12.4s broad	—	2.6s	2.1s 3H 2.0s 3H	12.4d (8.2)	5.9st + D_2O d (8.2)	5.8–4.8m 3H 4.3–3.4m 2H
E	$CDCl_3$	—	12.3s broad	—	2.6s	2.0s 12H	12.3d (8.2)	5.7m + D_2O d (9)	5.6–4.8m 4H 4.4–3.6m 2H
	(DMSO)–d_6	—	12.3s broad	—	2.6s	2.0s 12H	12.3d (8.2)	5.9m + D_2O d (9.5)	5.8–4.7m 4H 4.4–3.8m 2H
F	$CDCl_3$	3.6s	—	—	2.6s	2.3s 3H 2.1s 3H 2.0s 3H	12.4d (8.2)	5.8st + D_2O d (8.2)	5.6–4.7m 3H 4.4–3.2m 2H
	(DMSO)–d_6	3.5s	—	—	2.7s	2.1s 3H 2.0s 3H 1.9s 3H	12.2d (8.2)	5.9m + D_2O d (8.2)	5.8–4.6m 3H 4.3–3.6m 2H
G	$CDCl_3$	3.6s	—	—	2.7s	2.1s 12H	12.2d (8.2)	5.7m + D_2O d (9.5)	5.6–4.8m 4H 4.4–3.7m 2H
	(DMSO)–d_6	3.5s	—	—	2.7s	2.0s 12H	12.0d (8.2)	5.9m + D_2O d (9.5)	5.8–4.8m 4H 4.4–3.8m 2H

Protons H–1 and C_4–NH exchangeable by D.
s: singlet, d: doublet, st: pseudotriplet; m: multiplet.

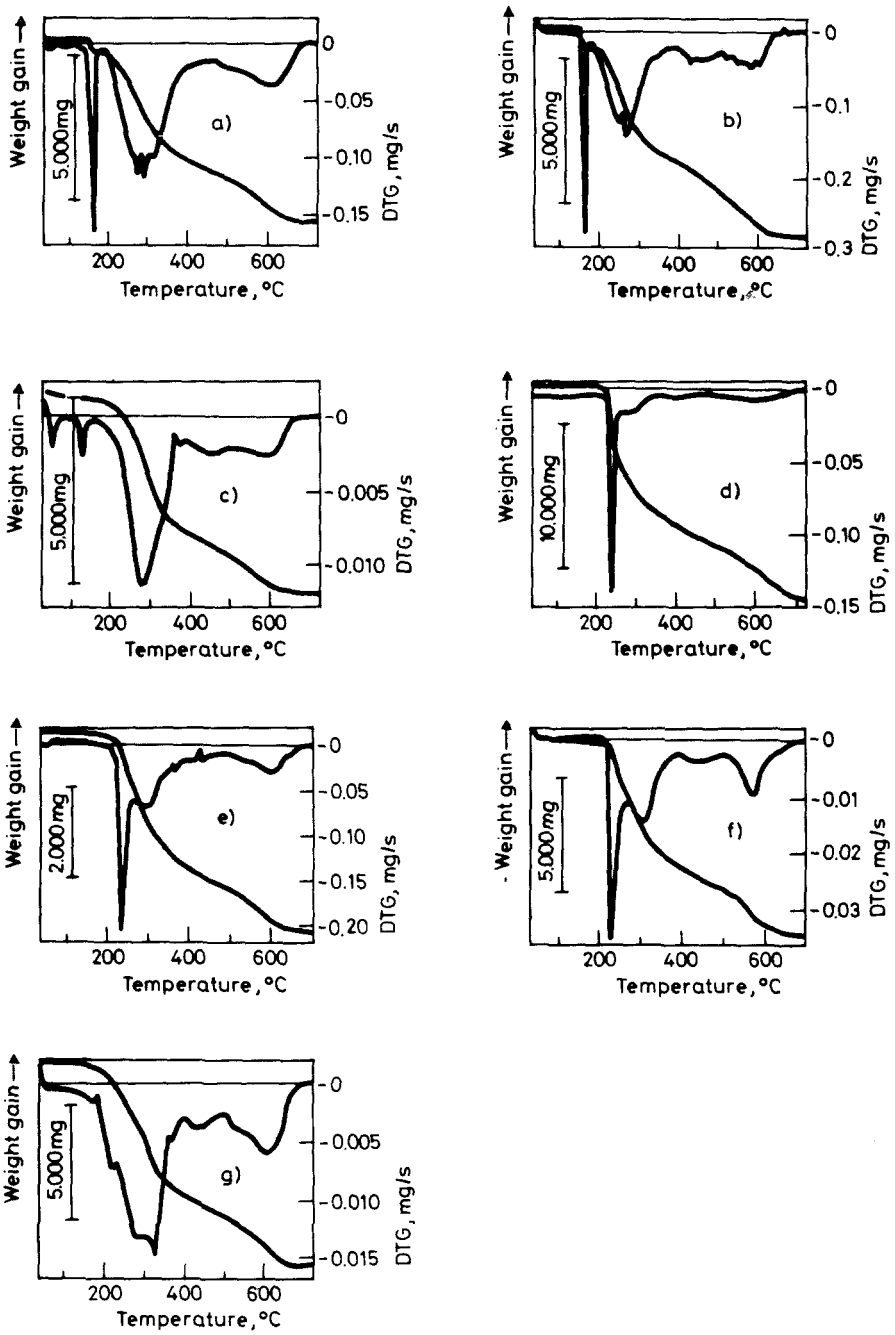

Fig. 1 TG plots

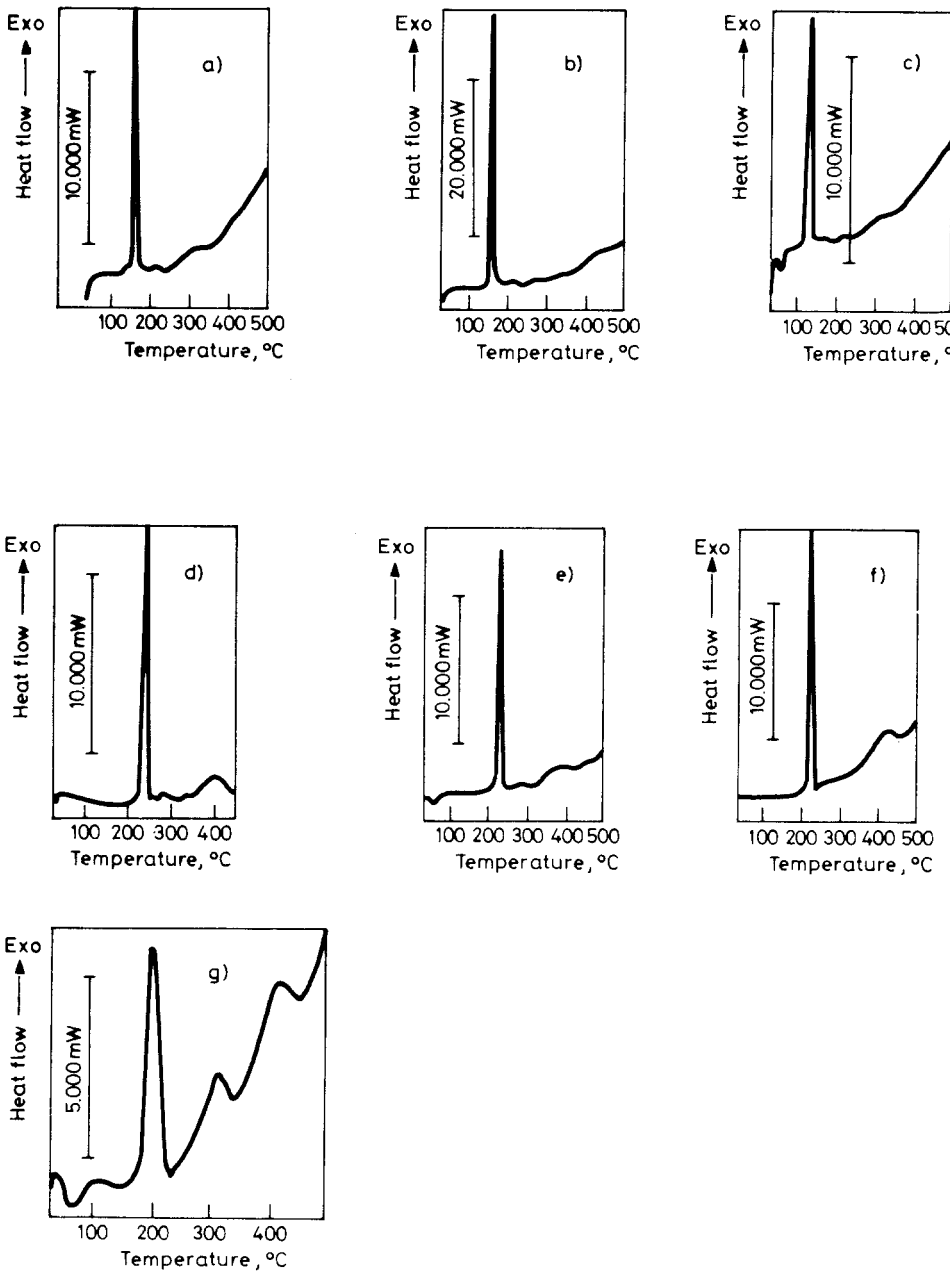

Fig. 2 DSC plots

Table 5 TG and DSC data on the compounds

Compound	Desolvation			Probable polymerization		Loss of acetylated sugar residues			Other effects, T, °C
	T, °C	wt. loss, %	ΔH, kJ·mol^{-1}	T, °C	ΔH, kJ·mol^{-1}	T, range	T, °C	ΔH, kJ·mol^{-1}	
A	—	—	—	120 endo	—	185–325	230, exo(w)	—	400, exo(br)
							240, endo(w)	—	
				165 exo	−103.97	170–350	310, exo(w)	—	
B	—	—	—	159.9 exo	−123.71	175–350	220, exo(w)	—	440, exo(br)
							240, endo(w)	—	
C	61.4, endo	1.3	14.04	130.6, exo	−120.55	225–350	230, exo	—	450, exo(br)
							300, exo	—	
D	—	—	—	—	—	200–370	230, exo(s)	—	400, exo(br)
							255, exo(w)	—	
							275, exo(w)	—	
E	58.2, endo	1.1	14.90	—	—	200–350	230, exo(s)	—	380, exo(br)
							290, exo(w)	—	
F	—	—	—	—	—	200–350	224, exo	−109.90	420, exo(br)
							260, exo(w)		
							320, exo		
G	65.0, endo	1.9	26.36	—	—	185–350	150, endo	26.88	415, exo(br)
							203, exo	−110.52	
							310, exo		

w: weak; s: sharp, br: broad.

this behaviour contrasts with that of the corresponding non-nitrosated homologues, which fuse at temperature values lower than 220° [9], and proves the role of the NO groups on C–5 in probable intramolecular hydrogen-bonding interactions in the compounds studied here.

The three compounds having O–CH_3 groups as exocyclic substituents on C–2 (compounds A, B and C) start their pyrolytic decompositions at considerably lower temperatures than do the remaining four compounds. For the above three compounds, these processes start with a slight weight loss (6.66% for A, 7.46% for B and 3.79% for C) at above 150°. In the DSC plots of these compounds, a very sharp exothermic effect (the energy of which is given in Table 5) accompanies the pyrolytic effects, suggesting that the partial combustion of the samples takes place. The resulting species are relatively unstable, their pyrolytic decomposition going on almost uninterruptedly. In an attempt to characterize these intermediate species, we recorded the IR and ^{1}H–NMR spectra of the compounds previously heated up to the end temperature of the first pyrolytic process.

From these data, the following features were established during the pyrolytic processes:

a) The non-occurrence of the ν(NO) stretching vibration bands in the IR spectra of the heated samples.

b) The shifting of the $\nu(C=C)+\nu(C=N)$ stretching vibration bands to higher wavenumbers.

c) The diminishing of the intensity of the ^{1}H–NMR signal corresponding to the O–CH_3 group (approximately half of the intensity of the signal for the unheated sample).

d) The splitting of the N(2)–CH_3 signals.

e) The probable shifting of the C(4)–NH signal to higher field values (above 4.6 ppm).

All these points taken together suggest the complete loss of the NO substituents during the process under study, i.e. breaking of the C(4)–NH...(NO) bridges, which explains the shifting of the C(4)–NH ^{1}H–NMR signal. On the other hand, point c) suggests the loss of the O–CH_3 in a certain proportion of the molecules (maybe half of them).

Thus, it could be suggested that the reaction of the resulting species probably gives rise to some polymeric species, whose characterization is very difficult via only the ^{1}H–NMR and IR techniques.

As stated before, the pyrolytic decomposition of the latter species continues almost uninterruptedly. At this point, the DSC and TG plots of the seven compounds are very similar, as shown in Figs 1 and 2; the seven TG curves show an abrupt weight loss which ends at about 350°.

The IR spectra of the corresponding residues of all the samples heated up to the

end temperature of the strong weight loss which characterizes these pyrolytic processes clearly show the loss of all the bands assignable to the acetate groups, and those of the sugar residues: ν(C=O) acetate, ν(C—O) acetate and ν(N—H). This proves that the pyrolysis starts with the loss and combustion of the acetylated sugar residues (except in the cases of compounds A, B and C, in which the processes follow the previously discussed polymerization processes). The DSC effects corresponding to these processes are detailed in Table 5.

After the loss of the acetylated sugar residues, the decomposition of the compounds goes on steadily, without stable intermediate species formation (see Fig. 1), becoming complete at temperatures about 650°, when no sample remains in the crucible. The absence of a stable intermediate meant that no data could be obtained about the mechanism of the final pyrolytic decomposition steps.

References

1 A. Block (Ed.), Chemistry, Biology and Clinical Uses of Nucleoside Analogues, New York Academy of Sciences, New York 1975.

2 R. M. Ottenbrite and G. B. Butler (Eds), Anticancer and Interferon Agents, Vol. 24, Dekker, New York 1984.

3 J. L. Rideout, D. W. Henry and M. Beacham (Eds), Nucleosides, Nucleotides and Their Biological Applications, Academic Press, New York 1983.

4 C. Nakayama, H. Machida and M. Saneyoshi, J. Carbohydr., Nucleosides and Nucleotides, 6 (1979) 295.

5 P. F. Torrence, G. F. Huang, M. W. Edwards, B. Bhoosnan, J. Descamps and E. Clercq, J. Med. Chem., 22 (1979) 316.

6 M. N. Hughes, The Inorganic Chemistry of Biological Processes, 2nd edn., Wiley, London 1981.

7 R. López, M. Nogueras, A. Sánchez, J. Negrillo and A. Bernalte, Thermochim. Acta, 91 (1985) 173.

8 A. Sánchez, M. Nogueras, R. López, M. Gutierrez and E. Colacio, Thermochim. Acta, 86 (1985) 199.

9 R. López, A. Sánchez, M. Nogueras, J. Negrillo and A. Bernalte, Thermochim. Acta, 96 (1985) 59.

10 R. Asenko, M. Melgarejo, C. Rodriguez, M. Nogueras and A. Sánchez, An. Quím., 79C (1983) 417.

11 C. Rodriguez, Thesis, University of Granada (1979).

12 A. Albert, J. Chem. Soc., (1962) 3129.

13 P. Lardenois, M. Selim and P. Selin, Bull. Soc. Chim. Fr., 5 (1971) 1958.

14 J. Kister, D. Bourn-Roubaud, L. Boucasse and J. Metzger, J. Spectrosc. Lett., 13(1) (1980) 1.

15 D. Bourn-Roubaud, J. Kister, L. Boucasse and J. Metzger, J. Spectrosc. Lett., 14(6) (1981) 431.

16 D. Pasto and Johnson, Determinación de Estructuras Orgánicas, Ed. Reverté, Barcelona, 1974, p. 109.

17 L. B. Clark and J. Tinoco, J. Am. Chem. Soc., 87 (1965) 11.

18 S. F. Mason, J. Chem. Soc., 2071 (1974).

19 M. Nogueras, A. Sánchez, R. Asenjo, M. Melgarejo, M. Rodriguez and C. Rodriguez, An. Quím., 80C (1984) 234.

20 R. Asenjo, M. Melgarejo, M. Nogueras, M. Rodriguez, C. Rodriguez and A. Sánchez, J. Nucleosides Nucleotides, 3(2) (1984) 207.

Zusammenfassung — Es wird über die Synthese, das spezifische optische Drehungsvermögen, die spektralen Eigenschaften (^{1}H–NMR-, sichtbare UV- und IR-Spectroskopie) sowie die thermische Kennzeichnung von sieben 4-(o-Azetyl)-glykopyranosylamino-5-nitrosopyrimidinderivaten berichtet. Mittels IR-Spektroskopie wurde die Einleitung des Mechanismus der pyrolytischen Zersetzung der Verbindungen untersucht.

Резюме — Приведен синтез, удельное оптическое вращение, спектральные данные (ПМР-, ИК- и спектроскопия в видимой области) и термические характеристики семи производных 4-(О-ацетил)-гликопиранозиламино-5-нитрозопиримидина. С помощью ИК спектроскопии установлен механизм начального пиролитического разложения этих соединений